

Electronic Supplementary Information

**Pushing the Boundaries: Enhancing TiO₂ Performance for
Hydrogen Evolution under Visible Light Photocatalysis by
Incorporating RuO₂**

Moses D. Ashie¹, Gayani Pathiraja², Shobha Mantripragada², Bishnu P. Bastakoti^{1*}

¹Department of Chemistry, North Carolina A&T State University, Greensboro, NC 27411, USA

²Department of Nanoscience, Joint School of Nanoscience and Nanoengineering, University of North Carolina at Greensboro, 2907 East Gate City Blvd, Greensboro, NC 27401, USA

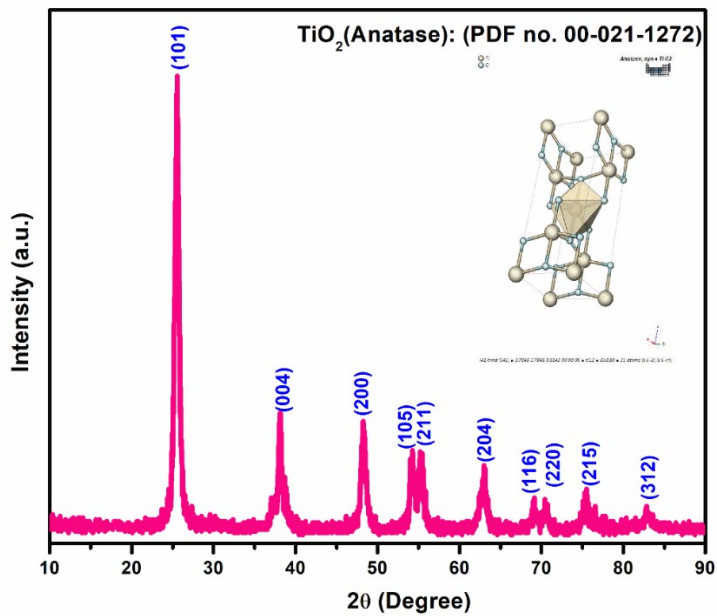


Fig. S1. XRD pattern anatase TiO_2 .

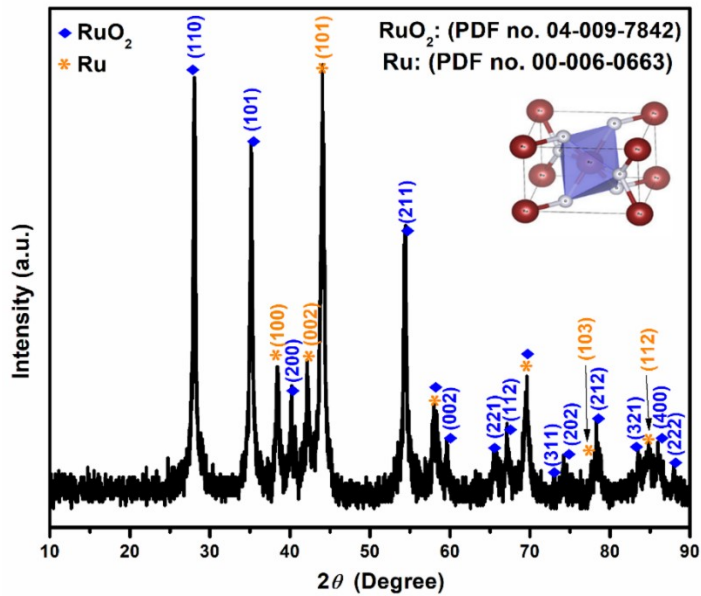


Fig. S2. XRD pattern of RuO₂.

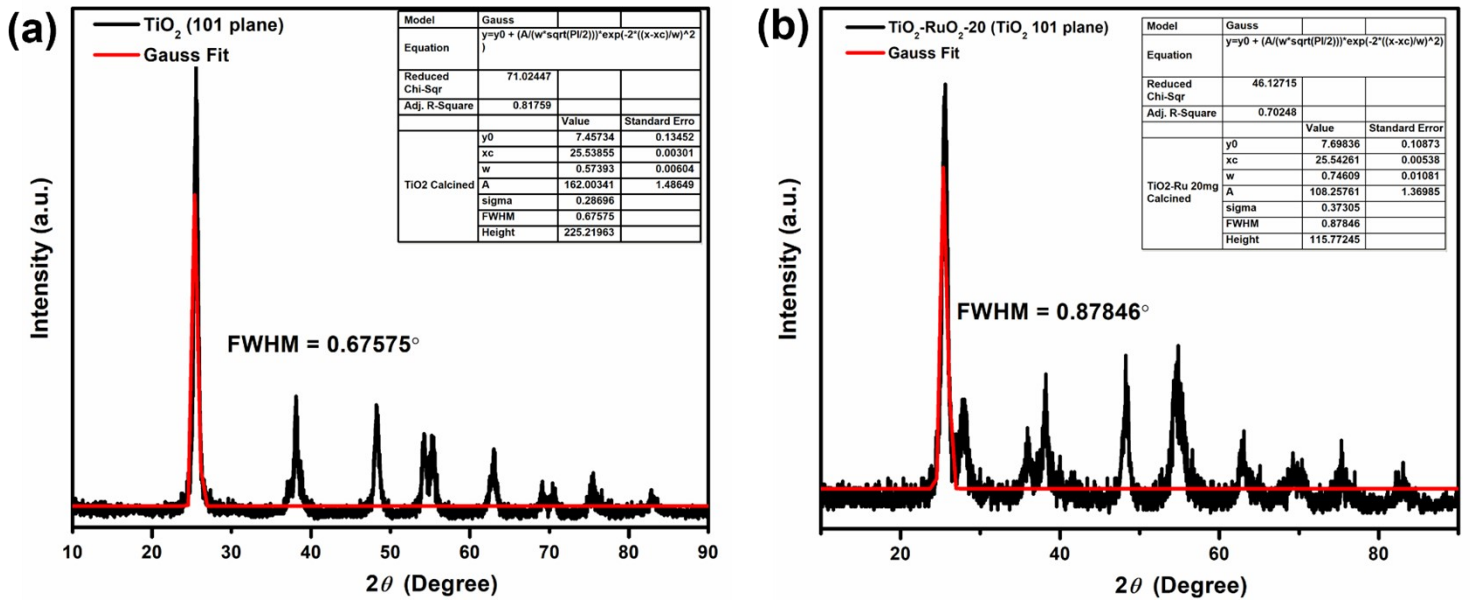


Fig. S3. Crystalline size determination of (a) TiO₂ only, and (b) TiO₂-RuO₂-20 samples calculated using the full width at half maximum (FWHM) of peaks from XRD patterns and Debye Scherrer equation.

$$D = \frac{K\lambda}{\beta \cos\theta}$$

Where: D is the mean crystallite size

λ is the X-ray wavelength

K is the shape factor (typically around 0.9)

β is the line broadening at half the maximum intensity (FWHM), in radians

Table S1. Summary of calculation of crystalline size of pristine TiO₂, pristine RuO₂, and synthesized TiO₂-RuO₂ composite samples.

Sample	FWHM (Degree)	FWHM (Radians)	Bragg's angle	Crystalline size (D)
TiO ₂ - Pristine	0.67575	0.011794	25.53	13.31053
RuO ₂ - Pristine	0.64128	0.011192	44.06	12.97287
TiO ₂ -RuO ₂ -10	0.75119	0.013111	25.48	11.74223
TiO ₂ -RuO ₂ -20	0.87846	0.015332	25.34	9.64816
TiO ₂ -RuO ₂ -40	0.75451	0.013169	25.42	11.46243
TiO ₂ -RuO ₂ -60	0.68464	0.011949	25.61	13.63861
TiO ₂ -RuO ₂ -100	0.86232	0.015050	25.46	10.15749

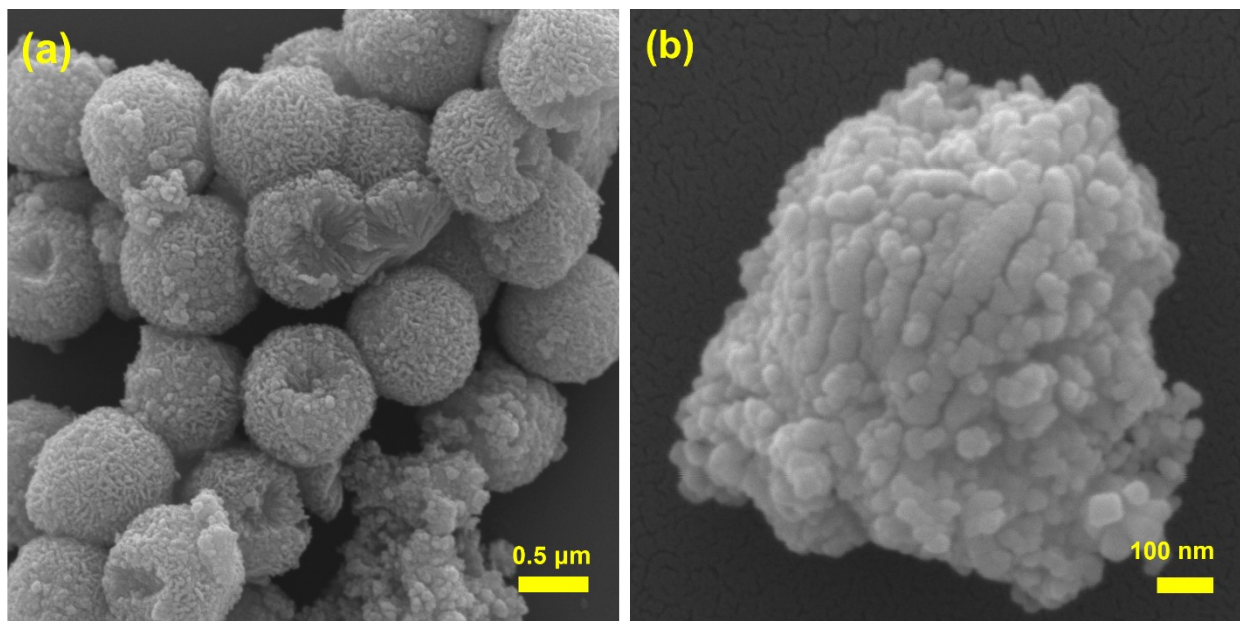


Fig. S4. FESEM image of a) pristine TiO_2 , and b) RuO_2 .

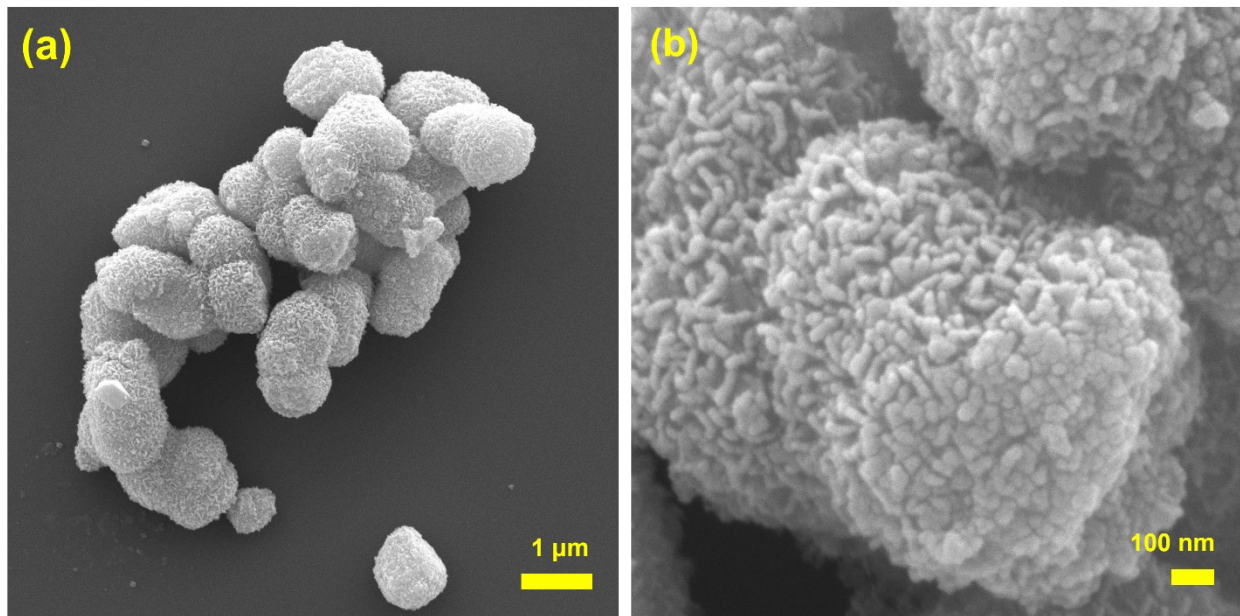


Fig. S5. SEM of TiO_2 - RuO_2 -10 composite sample.

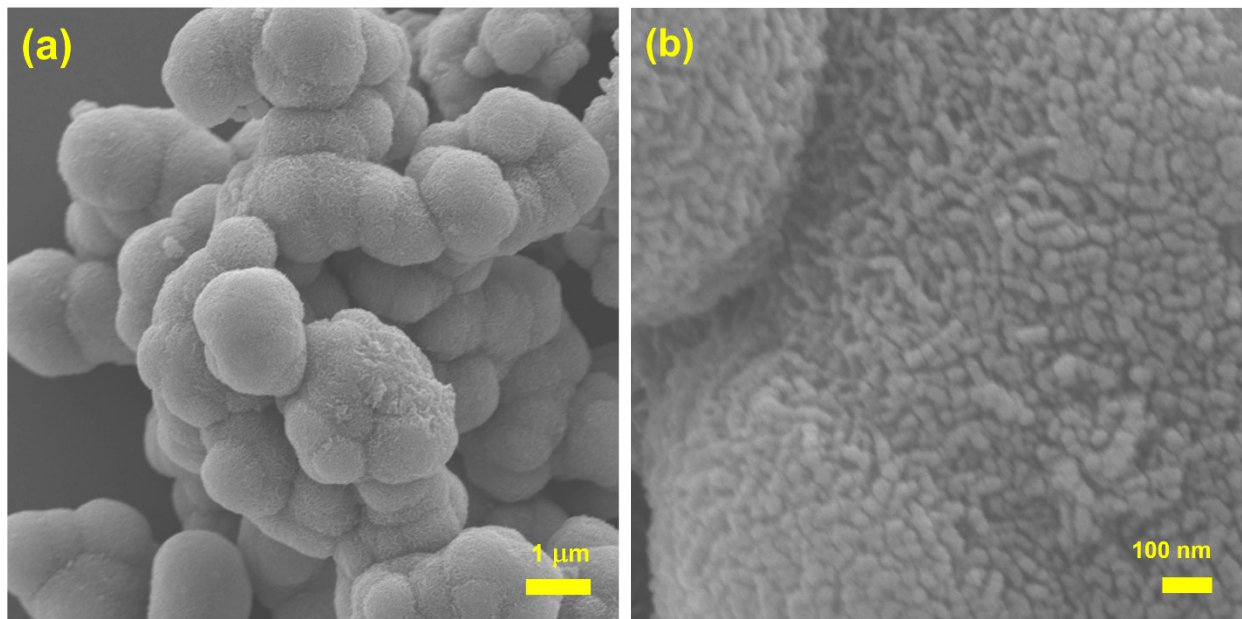


Fig. S6. SEM of TiO₂-RuO₂-20 composite sample.

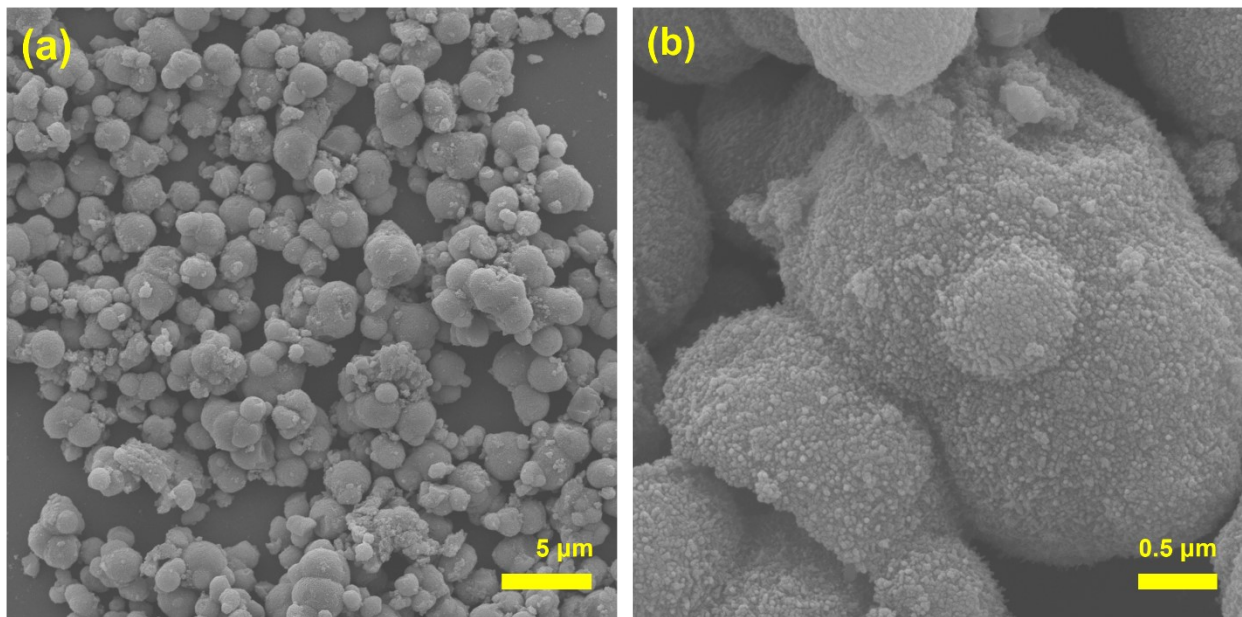


Fig. S7. SEM of TiO₂-RuO₂-40 composite sample.

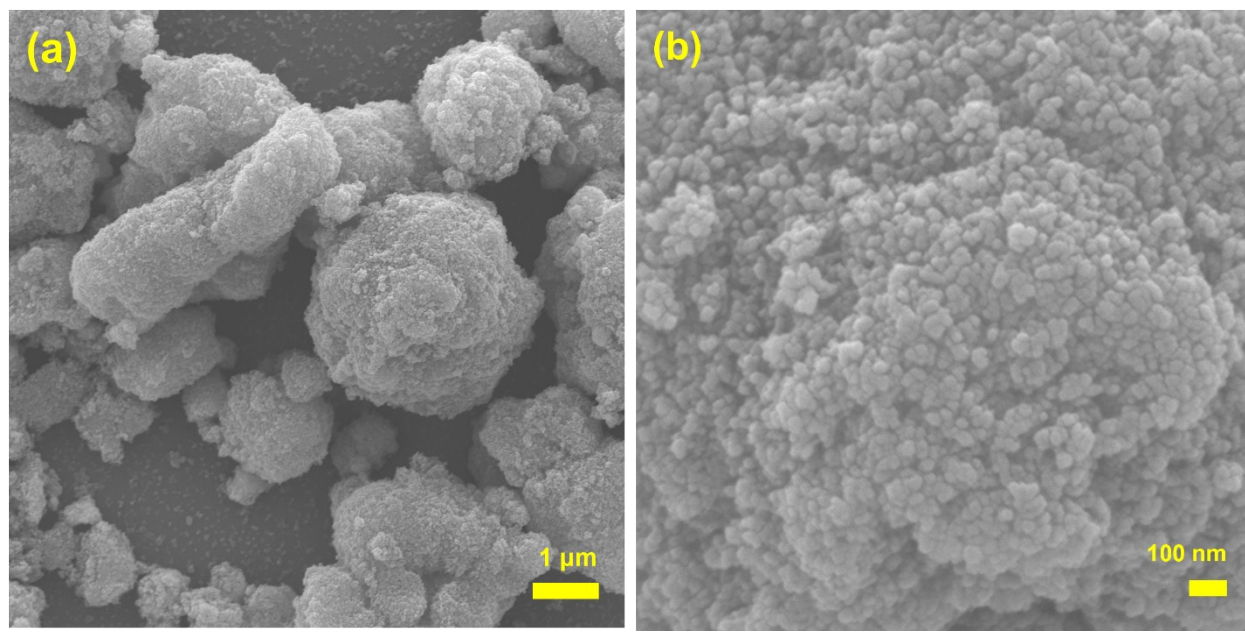


Fig. S8. SEM of TiO₂-RuO₂-60 composite sample.

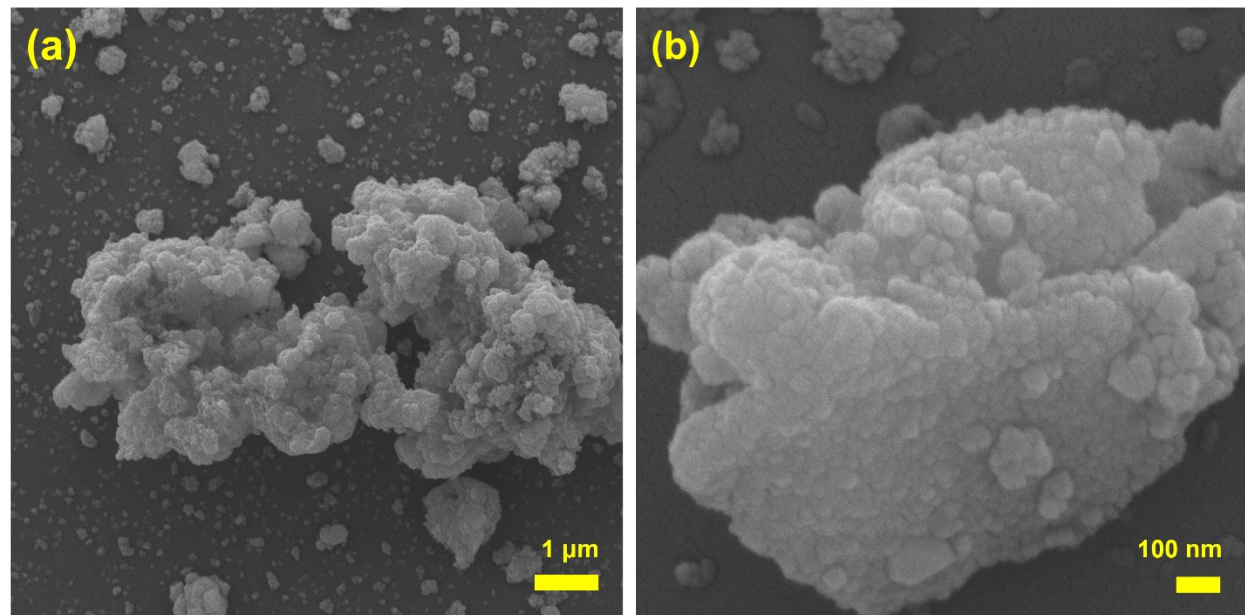


Fig. S9. SEM of TiO₂-RuO₂-100 composite sample.

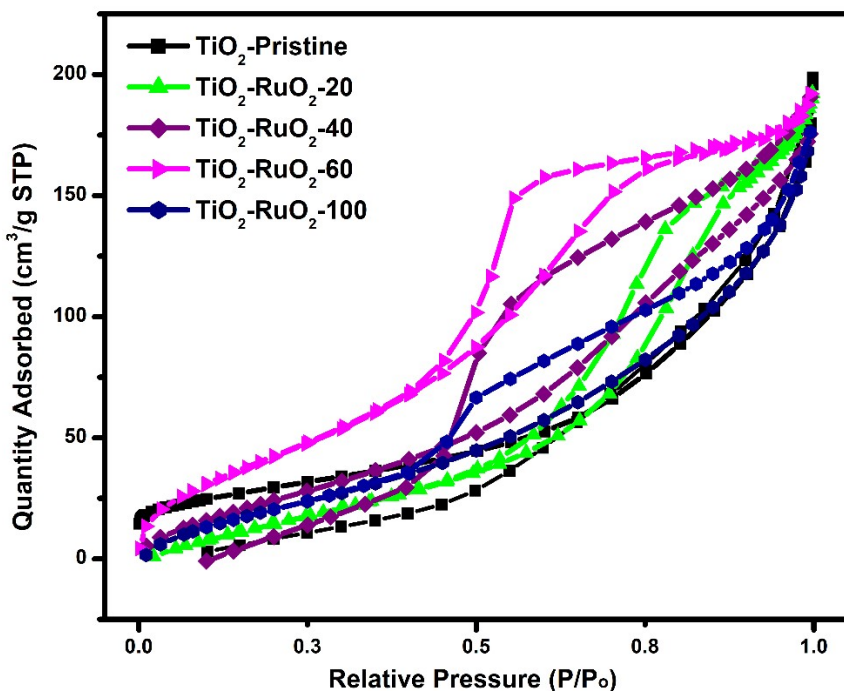


Fig. S10. Combined BET results of TiO₂, TiO₂-RuO₂-20, TiO₂-RuO₂-40, TiO₂-RuO₂-60, and TiO₂-RuO₂-100 samples.

Table S2. Summary of BET results of TiO₂, TiO₂-RuO₂-20, TiO₂-RuO₂-40, TiO₂-RuO₂-60, and TiO₂-RuO₂-100 samples.

SAMPLE	BET Surface Area (m ² /g)	BJH Pore Size (nm)
TiO ₂ -Pristine	106.99	9.04
TiO ₂ -RuO ₂ -20	115.42	8.38
TiO ₂ -RuO ₂ -40	95.97	6.1
TiO ₂ -RuO ₂ -60	155.22	4.64
TiO ₂ -RuO ₂ -100	101.9	7.12

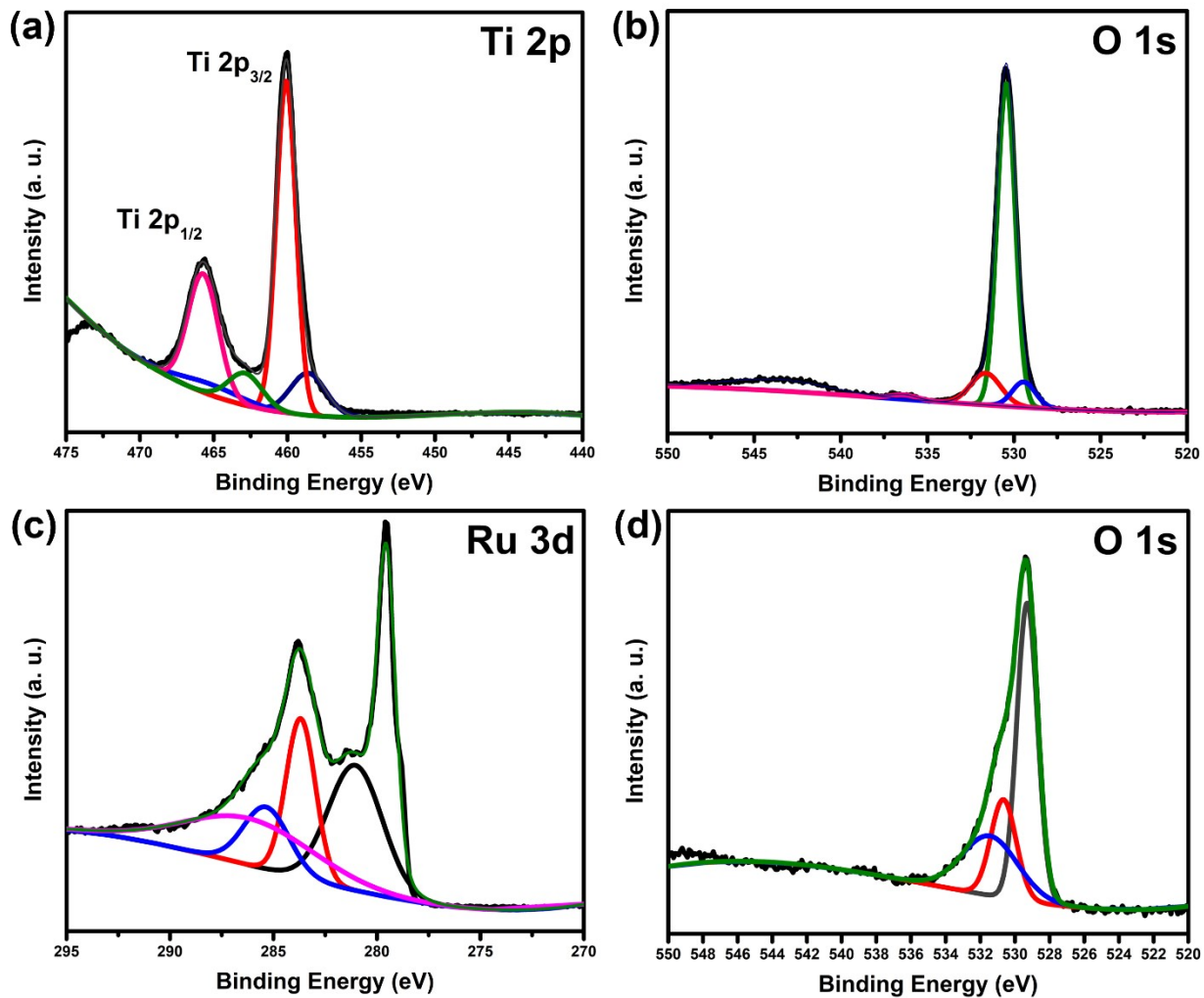


Fig. S11. XPS deconvoluted peaks for (a-b) pristine TiO_2 , and (c-d) pristine RuO_2 samples.

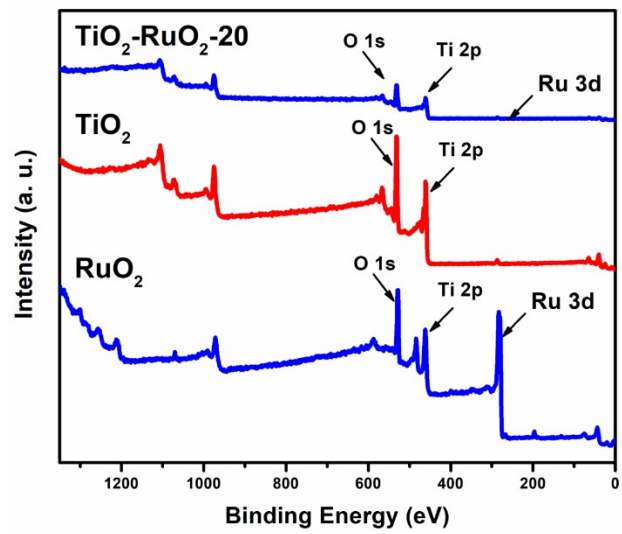


Fig. S12. XPS survey spectra of pristine TiO_2 , pristine RuO_2 and $\text{TiO}_2\text{-RuO}_2\text{-}20$ composite samples.

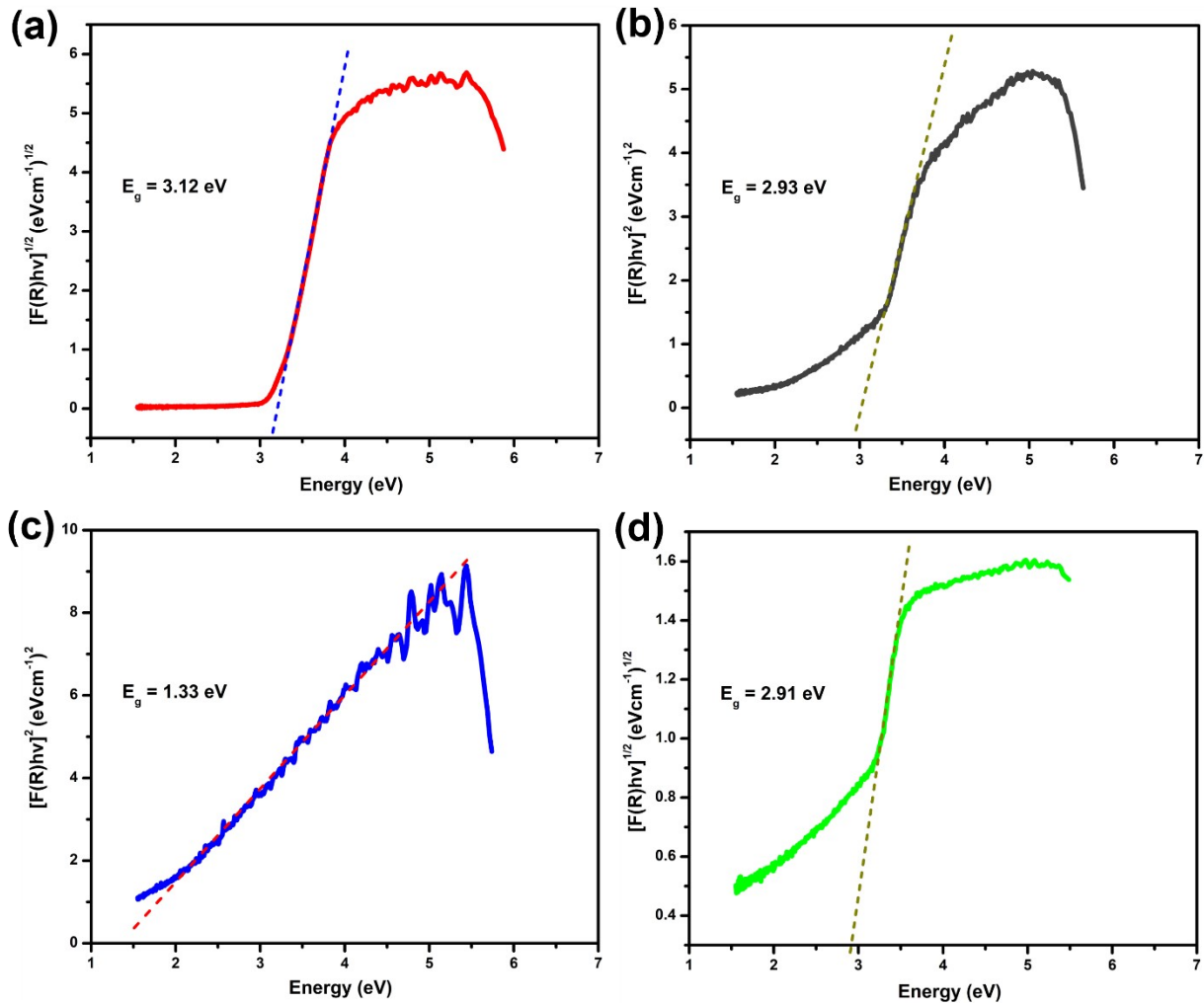


Fig. S13. Band gap of (a) Commercial TiO₂ (b) Synthesized TiO₂ (c) Synthesized RuO₂ and (d) Synthesized TiO₂-RuO₂-20 composite sample. Measurements taken using UV-Visible Diffuse Reflectance Spectroscopic (UV-Vis DRS) and diffuse reflectance data analyzed using Kubelka-Munk function $F(R_\infty)$ in a modified Tauc plot equation.

Kubelka-Munk function;

$$F(R_\infty) = \frac{(1 - R_\infty)^2}{2R_\infty}$$

Tauc equation given by;

$$(\alpha h\nu)^{1/n} = A(h\nu - Eg)$$

Where; i) the absorbance coefficient (α) in the Tauc equation is modified with the Kubelka-Munk function $F(R_\infty)$ to yield;

$$[F(R_\infty)h\nu]^{1/n} = A(h\nu - Eg)$$

ii) the diffuse reflectance data from DRS analysis is transformed using the Kubelka-Munk function and $[F(R_\infty)hv]^{1/n}$ plotted against hv .

iii) depends on the type of electronic transition:

$n = 1/2$ for direct allowed transitions

$n = 2$ for indirect allowed transition

$n = 3/2$ for direct forbidden transitions

$n = 3$ for indirect forbidden transitions

iv) hv is the photon energy

v) A is a proportionality constant

vi) E_g is the band gap energy of the synthesized samples estimated by extrapolation of the slope of the linear region to the x-axis

Table S3. Band gap results of pristine TiO_2 , pristine RuO_2 , and synthesized TiO_2 - RuO_2 samples.

Sample	Band Gap (eV)
TiO_2 -P25 (Commercial)	3.18
TiO_2 - Pristine	2.93
RuO_2 - Pristine	1.33
TiO_2 - RuO_2 10mg sample	2.88
TiO_2 - RuO_2 20mg sample	2.91
TiO_2 - RuO_2 40mg sample	2.69
TiO_2 - RuO_2 60mg sample	2.94
TiO_2 - RuO_2 100mg sample	2.93

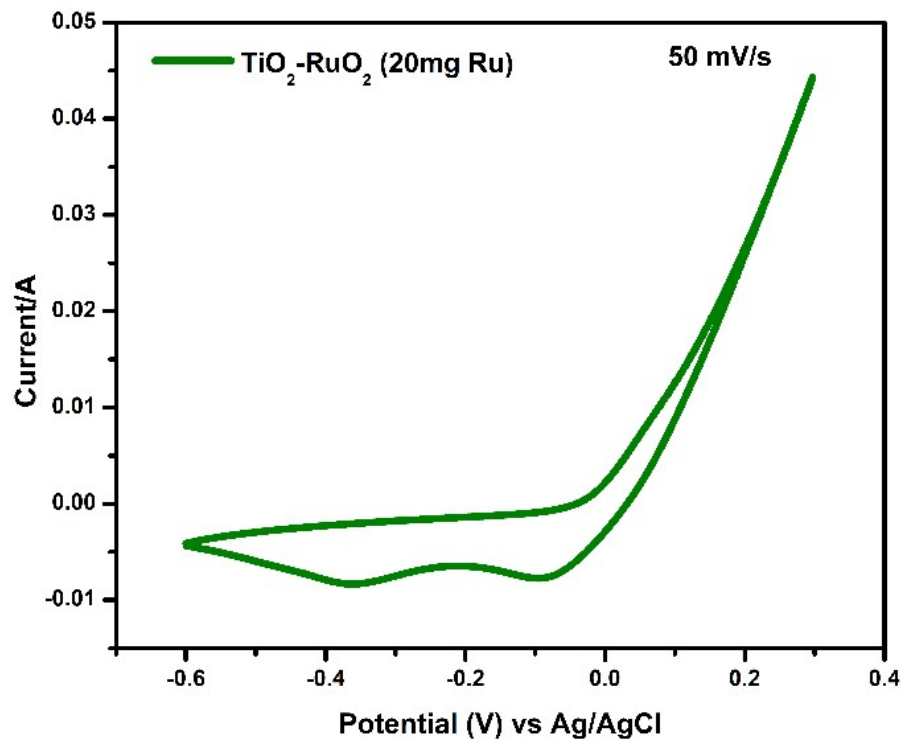


Fig. S14. Cyclic voltammetry of TiO₂-RuO₂-20 sample showing double reduction.

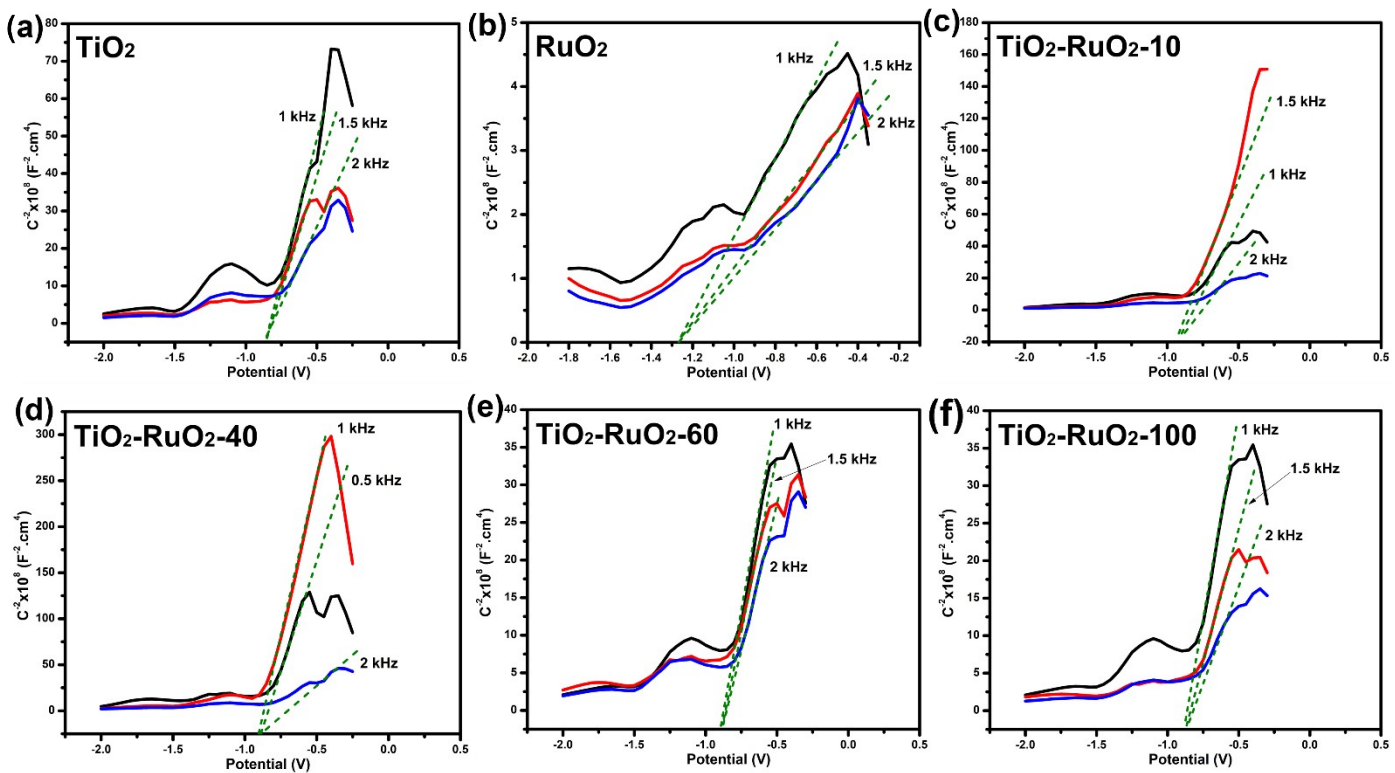


Fig. S15. Mott–Schottky plot for the electrochemical impedance potential investigation of TiO₂, RuO₂, TiO₂-RuO₂-10, TiO₂-RuO₂-40, TiO₂-RuO₂-60, and TiO₂-RuO₂-100 samples at different frequencies. Investigated in a three-electrode system using the synthesized material on a Cu substrate as working electrode, platinum electrode as a counter electrode, Ag/AgCl electrode as reference electrode, and 0.5 M Na₂SO₄ as electrolyte in ambient conditions.

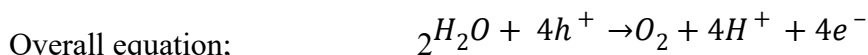
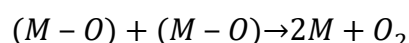
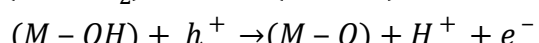
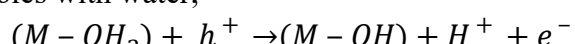
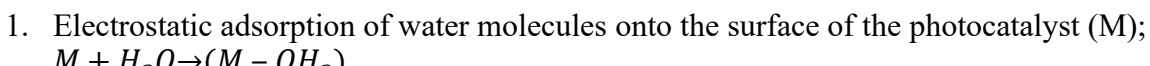
Table S4. Flat band potentials and donor densities of pristine TiO₂, pristine RuO₂, and synthesized TiO₂-RuO₂ samples.

SAMPLE	E(f _b) vs. Ag/AgCl	E(f _b) vs. NHE
RuO ₂	-1.27	-1.07
TiO ₂ -Pristine	-0.86	-0.66
TiO ₂ -RuO ₂ -10	-0.92	-0.72
TiO ₂ -RuO ₂ -20	-0.91	-0.71
TiO ₂ -RuO ₂ -40	-0.89	-0.69
TiO ₂ -RuO ₂ -60	-0.89	-0.69
TiO ₂ -RuO ₂ -100	-0.87	-0.67

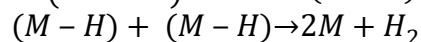
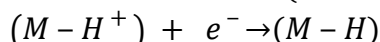
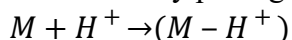
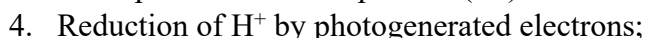
$$E_{fb} (\text{vs. NHE}) = E_{fb} (\text{vs. Ag/AgCl}) + 0.197 \text{ V}$$

Mechanism of water splitting

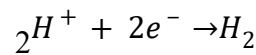
Oxidation:



Reduction:

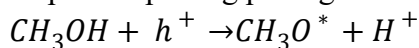


Overall equation;



Sacrificial agents:

5. Methanol used as sacrificial agent undergoes oxidation, releasing more protons. Also helps in capturing photogenerated holes to minimize electron-hole recombination.



The sacrificial agent readily donates electrons to react with the holes which will otherwise react to split water to produce oxygen.

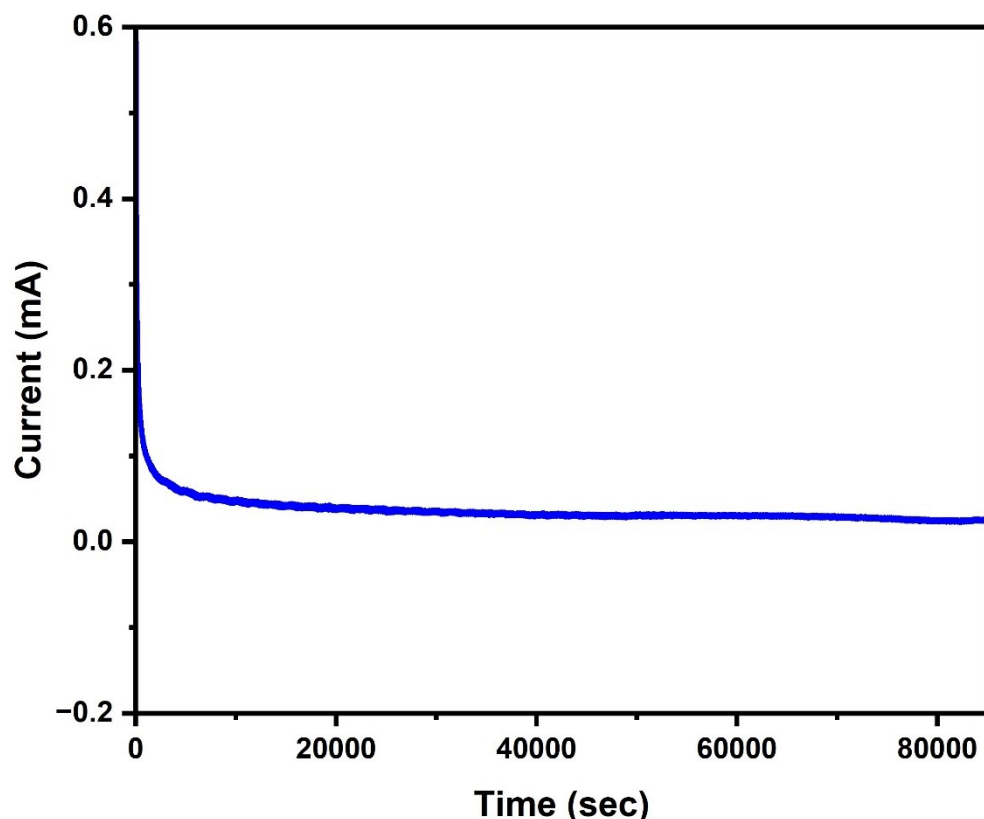


Fig. S16. TiO_2 - RuO_2 -20 sample showing good stability of electrode at 0.2 V applied potential for over 80000 s.

Material characterization after hydrogen evolution experiment

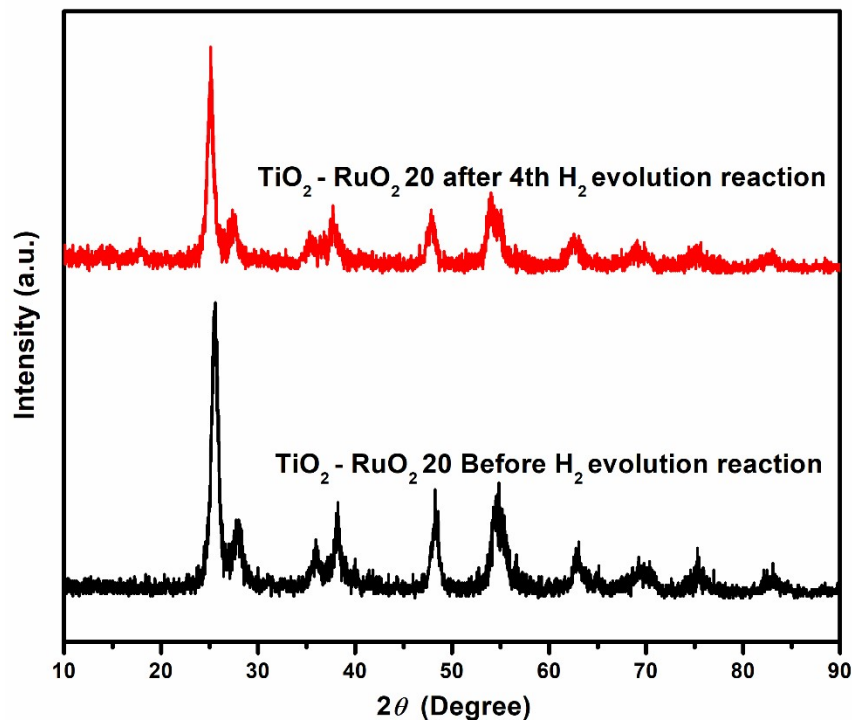


Fig. S17. Stability of TiO₂-RuO₂-20 samples after all cycles of hydrogen evolution activity. XRD pattern before and after hydrogen evolution experiments.

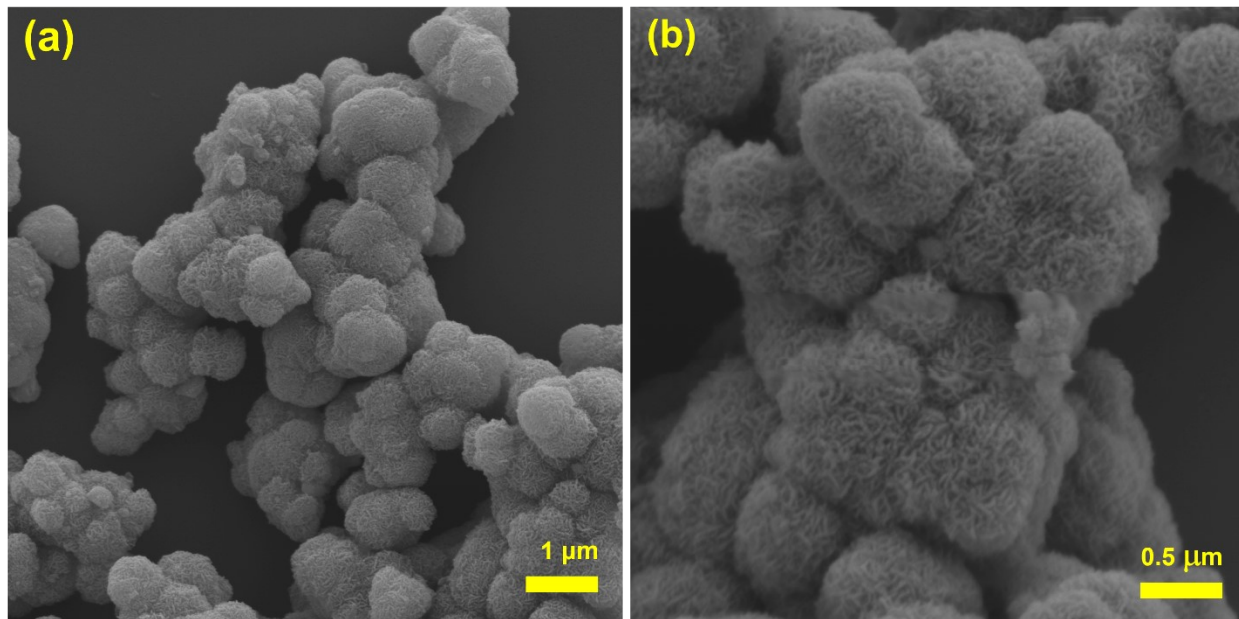


Fig. S18. SEM of $\text{TiO}_2\text{-RuO}_2\text{-20}$ sample after stability testing.

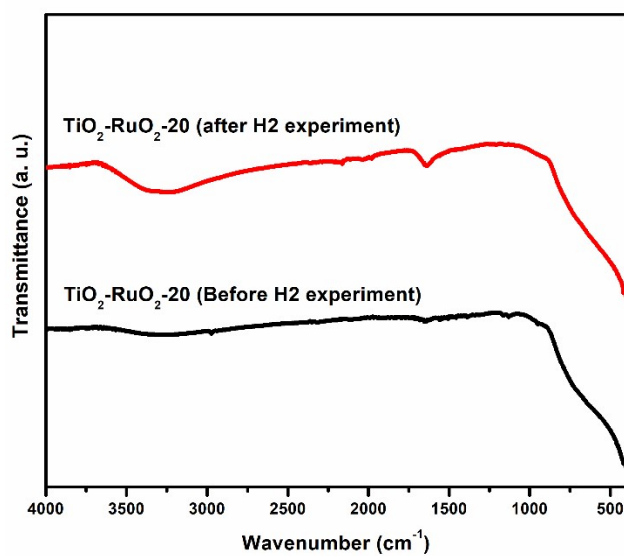


Fig. S19. FTIR of $\text{TiO}_2\text{-RuO}_2\text{-20}$ sample after stability testing. The peak observed at 1640 cm^{-1} is characteristic of C=O bond stretching^[5]. This can be attributed to the adherence of methanol (formaldehyde) produced from methanol as it acts as a sacrificial agent. The peak at about 3300 cm^{-1} can also be attributed to O-H stretching vibrations^[5]. This confirms that our material is highly stable since these molecules can be eliminated by annealing. Satellite peaks observed in XPS after stability testing can also be attributed to the presence of these molecules.

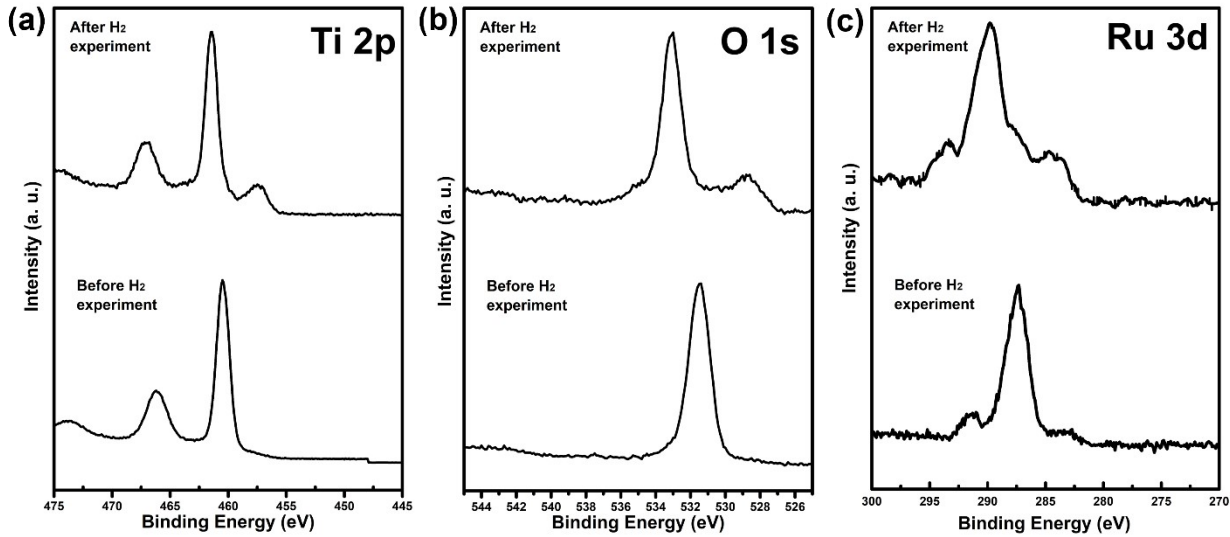


Fig. S20. XPS spectra of $\text{TiO}_2\text{-RuO}_2\text{-20}$ sample before and after stability testing. Satellite peaks and shifting of peaks observed after stability testing can also be attributed to the adherence of products (mainly formaldehyde) from the scavenging process.

REFERENCES

1. Sakata, T.; Hashimoto K.; Kawai, T. Catalytic Properties of Ruthenium Oxide on N-Type Semiconductors under Illumination, *Journal of Physical Chemistry*, 1984, 88.22, 5214–5221
2. Nguyen-Phan; Thuy D.; Si L.; Dimitriy V.; Jordi L.; Jesús G.; Javier F. S. Visible Light-Driven H₂ Production over Highly Dispersed Ruthenia on Rutile TiO₂ Nanorods, *ACS Catalysis*, 2016, 6.1, 407–417
3. Juliya, A. P.; Abdul Mujeeb, V. M.; Sreenivasan, K. P.; Muraleedharan, K. Enhanced H₂ Evolution via Photocatalytic Water Splitting Using Mesoporous TiO₂/RuO₂/CuO Ternary Nanomaterial, *Journal of Photochemistry and Photobiology*, 2021, 8, 100076
4. Cao, B.; Guisheng, L.; Hexing L. Hollow Spherical RuO₂@TiO₂@Pt Bifunctional Photocatalyst for Coupled H₂ Production and Pollutant Degradation, *Applied Catalysis B: Environmental*, 2016, 194, 42–49
5. FTIR Functional Group Database Table with Search - InstaNANO;

<https://instanano.com/all/characterization/ftir/ftir-functional-group-search/>